



Thermal conductivities under high pressure in core samples from IODP NanTroSEIZE drilling site C0001

Weiren Lin

Kochi Institute for Core Sample Research, Japan Agency for Marine–Earth Science and Technology, 200 Monobe-otsu, Nankoku 783–8502, Japan (lin@jamstec.go.jp)

Also at Geology Course, Graduate School of Arts and Sciences, Kochi University, Kochi, Japan

Also at Key Laboratory of Tectonics and Petroleum Resources of Ministry of Education, China University of Geosciences, Wuhan, China

Osamu Tadai

Marine Works Japan Ltd., Nankoku 738–8502, Japan

Takehiro Hirose and Wataru Tanikawa

Kochi Institute for Core Sample Research, Japan Agency for Marine–Earth Science and Technology, 200 Monobe-otsu, Nankoku 783–8502, Japan

Manabu Takahashi

Institute for Geology and Geoinformation, National Institute of Industrial Science and Technology, Tsukuba 305–8567, Japan

Hideki Mukoyoshi

Marine Works Japan Ltd., Nankoku 738–8502, Japan

Masataka Kinoshita

Institute for Research on Earth Evolution, Japan Agency for Marine–Earth Science and Technology, Yokosuka 237–0061, Japan

[1] We examined the effects of high pressure on thermal conductivity in core samples from the slope–apron facies and the upper part of the accretionary prism at site C0001 of the NanTroSEIZE drilling program and in other samples of five terrestrial rock types. Thermal conductivity clearly increased with increasing pressure for both wet (water saturated) and dry samples. We determined the rate of thermal conductivity change of the NanTroSEIZE sediments to be $0.014 \text{ Wm}^{-1}\text{K}^{-1}/\text{MPa}$ when pressure was increased, and $0.01 \text{ Wm}^{-1}\text{K}^{-1}/\text{MPa}$ when pressure was decreased. Using the rate determined for decreasing pressure, we estimated that thermal conductivities measured at atmospheric pressure rather than at in situ pressure may be underestimated by 7% for a core sample from around 1 km depth and by 20% for a core sample from around 3 km depth. In general, the rate of thermal conductivity change with pressure showed a positive correlation with porosity. However, the relationship of the rate of thermal conductivity change to porosity is also dependent on the fabric, mineral composition, and pore structure of the sediments and rocks. Furthermore, for two sandstones we tested, the effect of pressure on thermal conductivity for dry samples was greater than that for wet samples.

Components: 6600 words, 9 figures.

Keywords: NanTroSEIZE; high pressure; thermal conductivity.

Index Terms: 7240 Seismology: Subduction zones (1207, 1219, 1240); 8130 Tectonophysics: Heat generation and transport; 8194 Tectonophysics: Instruments and techniques.

Received 29 November 2010; **Revised** 7 April 2011; **Accepted** 8 April 2011; **Published** 24 June 2011.

Lin, W., O. Tadai, T. Hirose, W. Tanikawa, M. Takahashi, H. Mukoyoshi, and M. Kinoshita (2011), Thermal conductivities under high pressure in core samples from IODP NanTroSEIZE drilling site C0001, *Geochem. Geophys. Geosyst.*, *12*, Q0AD14, doi:10.1029/2010GC003449.

Theme: Theme: Mechanics, Deformation, and Hydrologic Processes at Subduction Complexes, With Emphasis on the Nankai Trough Seismogenic Zone Experiment (NanTroSEIZE) Drilling Transect

1. Introduction

[2] The Nankai Trough Seismogenic Zone Experiment (NanTroSEIZE) is a comprehensive scientific drilling program that commenced in 2007 in the Nankai trough region, southwestern Japan, under the IODP [Kinoshita *et al.*, 2006]. Convergence of the Philippine Sea and Eurasian plates in this region has caused M8-class great earthquakes with recurrence intervals of 100–200 years. A plausible geophysical model of the subduction zone is critical to understanding the cycle of earthquake occurrences, coseismic fault rupture, and the accumulation and release of seismic energy [Lallemand and Funiciello, 2009]. Developing such a model by determining the physical properties under in situ conditions, including thermal conductivity, of materials retrieved from depth is an important scientific objective of NanTroSEIZE. Thermal conductivity is an important parameter for estimations of the frictional heating that accompanies fault rupture [Lachenbruch, 1980; Kano *et al.*, 2006; Tanaka *et al.*, 2006] and of heat flow and thermal regimes [Hyndman *et al.*, 1995; Wang *et al.*, 1995; Kinoshita *et al.*, 1996; Harris and Wang, 2002; Villinger *et al.*, 2002; Yamano *et al.*, 2003]. In addition, knowing the diffusivity is important for understanding transient thermal processes and knowing the thermal conductivity is important for knowing the thermal diffusivity [Goto *et al.*, 2005].

[3] The physical properties of sedimentary rocks, including thermal conductivity, are dependent on pressure and temperature [Schön, 1998a], so in situ pressure and temperature conditions should be simulated in laboratory measurements of the thermal conductivity of core samples from great depths. Many previous studies on thermal conductivity at high pressure were found for hard rocks even up

to a very high pressure of more than 1 GPa [e.g., Horai and Susaki, 1989; Kukkonen *et al.*, 1999; Osako *et al.*, 2004; Xu *et al.*, 2004; Pribnow *et al.*, 1996; Seipold and Huenges, 1998], but a few literatures for ocean sediments are available [e.g., Morin and Silva, 1984].

[4] An ultradeep well is planned at site C0002 during Stage III of NanTroSEIZE commencing in 2012. This well will aim to penetrate the seismogenic asperity of the 1944 Tonankai earthquake in the Nankai subduction zone off southwestern Japan. To date, no data from laboratory tests on the effect of pressure on thermal conductivity of sediments and sedimentary rocks from the Nankai trough region have been published, and there appears to have been no research on their thermal conductivity under high-pressure conditions.

[5] We developed an apparatus capable of measuring the thermal conductivity of sedimentary rocks at pressures up to 200 MPa, corresponding to lithostatic pressure at 8 km depth, which is deeper than the maximum drilling depth planned for NanTroSEIZE. This apparatus will be further modified in the future to allow measurement of thermal conductivity at high temperatures.

[6] For this study, we used two core samples from the Nankai subduction zone at site C0001 [Ashi *et al.*, 2008]: one from the slope–apron facies and one from the upper accretionary prism. We examined the variation of thermal conductivity of these wet samples at pressures simulating those at their original depth and at greater depths. We also performed high-pressure thermal conductivity tests on several other terrestrial rock samples including a granite, three sandstones, and a welded tuff. Our results suggest that to determine the in situ thermal conductivity of core samples from deep wells, it is

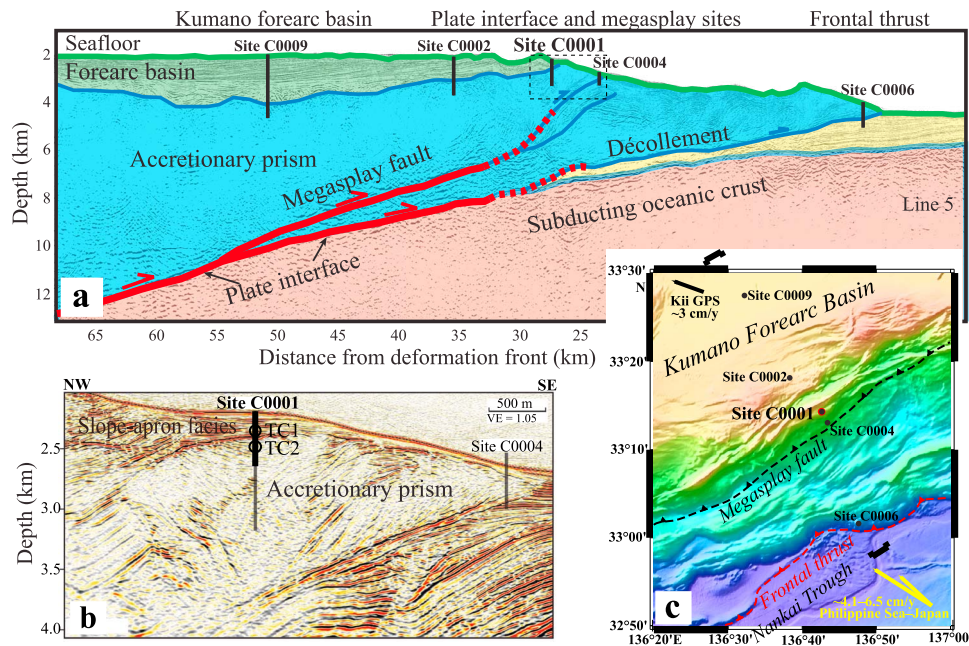


Figure 1. Location and geological setting of NanTroSEIZE site C0001 and the other sites. (a) Interpreted seismic section [after Park *et al.*, 2002] showing relationship of NanTroSEIZE drilling sites to geological structure in the Nankai subduction zone. The dashed rectangle shows the area of Figure 1b. (b) Seismic reflection profile through site C0001 showing locations of core samples TC1 and TC2 used in this study (modified from Expedition 315 Scientists [2009]). The thick black line at drill site C0001 shows the interval cored during Expedition 315; the narrow gray line shows the interval drilled without coring during Expedition 314. (c) Bathymetric map of the NanTroSEIZE region showing drilling sites (modified from Lin *et al.* [2010a]) in relation to the megasplay fault and frontal thrust [Moore *et al.*, 2007]. Brackets show location of the cross section in Figure 1a. Yellow arrows show the far-field convergence vectors between the Philippine Sea plate and Japan [Heki and Miyazaki, 2001]; black arrow shows far-field plate motion vector based on geodetic survey data of Heki and Miyazaki [2001].

important that experimental measurements are taken at high pressures that simulate the conditions at the depths from which the samples came.

2. Core and Rock Samples

[7] More than 10 vertical boreholes have been drilled along the NanTroSEIZE transect (Figure 1), which is approximately orthogonal to the axis of the Nankai Trough and hence orthogonal to the tectonic plate boundary. We measured the high-pressure thermal conductivity of two samples from above a megasplay fault at site C0001. The upper sample (TC1, 183.33 m below seafloor, core C0001F-9H-3) was from lithological Unit I-B, which was defined as slope–apron facies. The other sample (TC2, 293.13 mbsf, C0001H-7R-6) was from Unit II in the upper part of the accretionary prism (Figure 1b) [Expedition 315 Scientists, 2009]. Sample TC1 was of late Pliocene to early Pleistocene age and sample TC2 was of early Pliocene age. Both samples were coherent silty muds of similar porosity (56–57%) and wet bulk density

(1.74–1.77 g/cm³). These two core samples were kept at original water content state which was the water saturated state. This “wet state” was confirmed by water–content and porosity measurements using small pieces cut from the same cores as the thermal conductivity samples.

[8] To test our high-pressure thermal conductivity measurement apparatus, and to examine the general relationships of thermal conductivity to confining pressure for various rocks, we also performed high-pressure tests on five other rock types and on a sample of fused silica. The rock samples were fine-grained Aji Granite (porosity 0.85%, wet bulk density 2.64 g/cm³ determined by the buoyancy method [Franklin, 1979]) from Kagawa, Japan; Rajasthan sandstone (10.6%, 2.45 g/cm³) from India; Shirahama sandstone (13.5%, 2.43 g/cm³), a Miocene rock from Kii Peninsula, which is approximately 120 km from site C0001; Berea sandstone (19.7%, 2.31 g/cm³) from Ohio, USA; and Tago welded tuff (31.9%, 2.03 g/cm³) from the Miocene Oya formation in Tochigi, Japan.

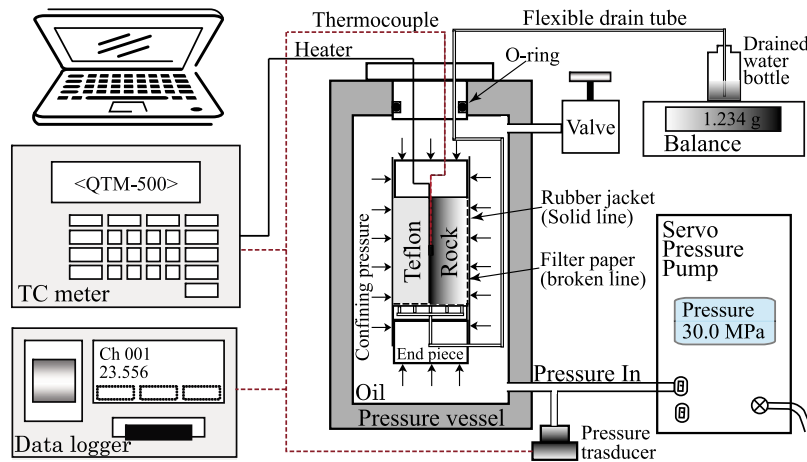


Figure 2. Schematic diagram of the apparatus developed in this study for measurement of thermal conductivity under high-pressure conditions. The system consists of a hydrostatic pressure vessel with a servo-controlled pump that provides pressures up to 200 MPa, a wire-type line source sensor in the pressure vessel, a thermal-conductivity meter (QTM-500) to measure thermal conductivity from the wire sensor, an electrical balance to monitor drained water mass for calculation of volumetric deformation of wet samples associated with consolidation, and a data logger.

[9] Basically we prepared dry samples for the five terrestrial rocks dried in an oven at 110°C for more than 24 h and then moved into a dried desiccator for cooling to room temperature and keeping dry state until thermal conductivity tests [Franklin, 1979]. To compare the pressure effects on thermal conductivity for dry and wet samples, we also prepared fully water-saturated samples for Shirahama and Berea sandstones. The samples were soaked in ion-exchanged water in a vacuumed desiccator for more than three days for water saturation just before the thermal conductivity test.

3. Measurement Method of Thermal Conductivity

[10] The commercial thermal conductivity meter QTM-500 we used is based on transient heating of a half-space sample by a line source [Sass *et al.*, 1984; Galson *et al.*, 1987]. This approach is usually used for tests at atmospheric pressure with a cased box-type line source sensor probe [Horai, 1981; Sass *et al.*, 1984]. For high-pressure thermal conductivity measurements, it is necessary to place the sample and sensor in a high-pressure vessel. Because commercial box-probe cannot be used at high pressures, we instead used a wire-type line source sensor consisting of a line heater and a thermocouple to measure temperature changes at the center of the line heater during heating.

[11] In our apparatus (Figure 2), the wire sensor was placed between a halved cylindrical rock

sample (50 mm diameter, 100 mm length) and a matching piece of Teflon ($0.29 \text{ Wm}^{-1}\text{K}^{-1}$) of the same dimensions. We installed the wire sensor through a dielectric endpiece at the top of the sample, from where it ran between the sample and the Teflon. We used the endpiece at the bottom of the sample to allow pore water to drain from the sample and to control pore pressure. Filter papers were placed between the rubber jacket and the rock sample and between the bottom endpiece and the sample to promote drainage of pore water. For this study, we did not control pore pressure (i.e., we ran all of the tests with pore pressure equal to atmospheric pressure for both dry and wet samples), but estimated the volumetric change of the wet samples by measuring the mass of drained water with an electric balance (10^{-3} g resolution).

[12] This sensor type of line source measures the thermal conductivity in a direction perpendicular to the line source, i.e., core sample axis in our sample assembly. If the core sample was taken from vertical drilling, the measured thermal conductivity is in horizontal direction. If it is possible to make up two or more samples from the same rock in the same dimension (a halved cylindrical sample with 50 mm diameter and 100 mm length) but in different directions, we can examine anisotropy of thermal conductivity under high pressure of the rock. In case of drill core, however, length of a sample taken in a direction perpendicular to the drill core axis might be limited by the diameter of the core. If the length is less than 10 cm, it is necessary to develop a new sample assembly for smaller sample and to conduct

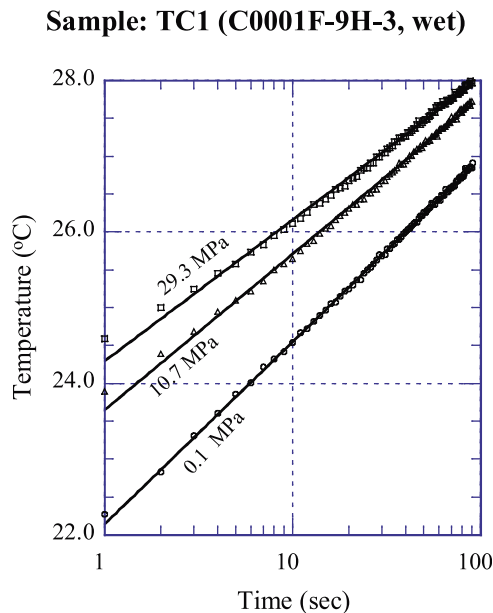


Figure 3. Examples of thermal conductivity measurements for NanTroSEIZE sample TC1 (wet) at three different confining pressures. The gradient of each data series at semilog scale is inversely proportional to the thermal conductivity.

related fundamental pretests including calibration tests before the thermal conductivity tests.

[13] We placed the sample assembly in a hydrostatic high-pressure vessel with an oil medium and a servo-controlled pressure pump with a maximum pressure of 200 MPa at room temperature (around 23°C). By assuming a water depth of 2 km (almost the same as that at site C0001) and an average density of around 2.25 g/cm³ along the vertical profile of sediments and rocks, the maximum pressure of 200 MPa simulates a lithostatic pressure regime equivalent to 8 km depth below the seafloor.

[14] For thermal conductivities measured with transient line source devices such as the QTM-500, the lower the thermal conductivity of the test sample, the steeper the increase of temperature during heating. Thus, the apparent thermal conductivity (λ_{app}) for the rock and Teflon combination we used can be calculated as

$$\lambda_{app} = KQ[\ln(t_2) - \ln(t_1)]/4\pi(T_2 - T_1), \quad (1)$$

where K is a constant dependent on the measurement apparatus, Q is the quantity of heat, and T_1 and T_2 are temperatures at times t_1 and t_2 , respectively, during transient heating. Our high-pressure measurements showed an almost linear relationship at semilog scale between temperature and heating

time (Figure 3). The gradient decreased as confining pressure increased, indicating that apparent thermal conductivity increased with increasing confining pressure. We used the temperature data ranged between 20 and 90 s which are more stable than in the early part of 0–20 s for calculating apparent thermal conductivity. By using a calibration curve derived from several standard samples, the thermal conductivity of the rock sample can be determined from the apparent thermal conductivity.

[15] To examine precision (reproducibility) of measured thermal conductivity values by our high-pressure thermal conductivity measurement apparatus, we conducted the measurements for a fused silica specimen at five pressure steps in increasing confining pressure run and one step in decreasing pressure run. At each confining pressure step, we repeated the measurements 11–14 times but rejected the first measured value because the first measurement in the day looks to be usually bigger than the following measurements. After one measurement, we wait 30 min approximately before the next measurement because the line source heater makes the temperature of sample to rise higher than environmental temperature. The average values of measured thermal conductivities at the six pressure steps were within 1.50–1.52 Wm⁻¹K⁻¹; and the standard deviations were the same 0.01 Wm⁻¹K⁻¹ for all the six steps (Figure 4). Thus, the relative standard deviations (coefficient of variation) are less than 1% for all the pressure steps. As a result, this parameter is much less than 5% that the manufacturer of the thermal conductivity meter gave as both “reproducibility” and “accuracy.” We also measured three standard samples with given thermal conductivity values by using the wire-probe sensor at atmospheric environment; and recognized that the accuracy by the thermal conductivity meter and the wire-probe sensor was less than 5%.

[16] The average values of thermal conductivity showed a small increasing with increasing confining pressure because better closeness between the combination of sensor, fused silica and the Teflon under higher pressures, but the change with pressure was very limited (Figure 4). In addition, no hysteresis was recognized during the cycle of increasing and decreasing confining pressure.

4. Thermal Conductivities at High Pressure

[17] We measured thermal conductivities of the NanTroSEIZE core and the terrestrial rock samples

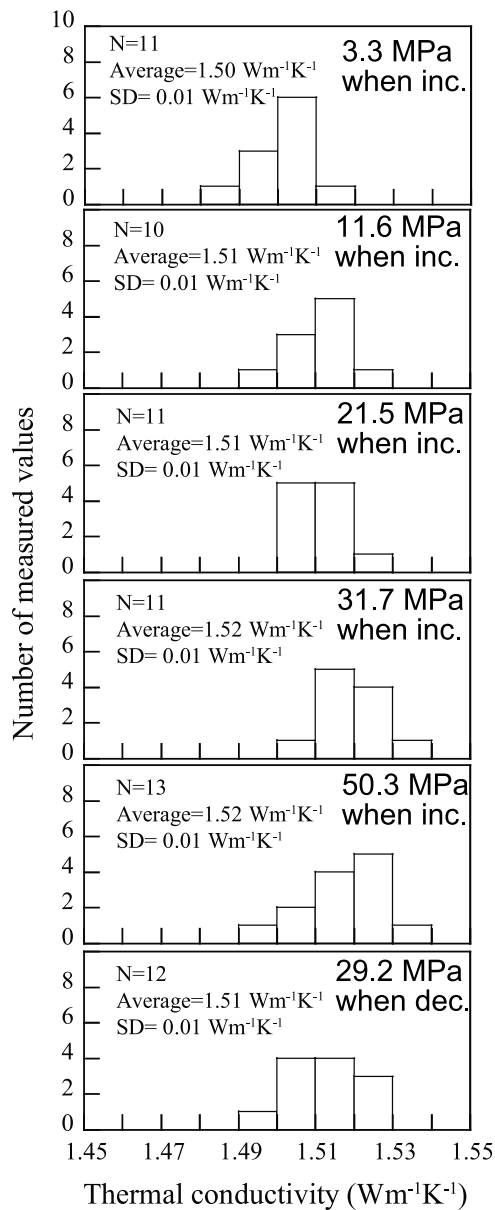


Figure 4. Histograms and statistical parameters of measured thermal conductivity values of fused silica under six confining pressure steps. N is the number of measured values; Average shows the arithmetic average value; SD means the standard deviation. Pressure values in right top shows the confining pressure; but inc. and dec. mean the measurements were performed during increasing and decreasing confining pressure, respectively.

for both increasing and decreasing stepwise changes of confining pressure, simulating subsidence and uplift, respectively. At each step of increasing pressure, the samples contracted (consolidated); for each step of decreasing pressure, the samples expanded (Figure 5, sample TC1). At each step, we kept the confining pressure constant over several hours after stepwise pressure loading or unloading; and then

measured thermal conductivity of the samples two or three times before proceeding to the next pressure step.

4.1. The NanTroSEIZE Samples

[18] For sample TC1, we measured thermal conductivity over a period of three days at seven confining pressure steps including 0.1 (atmospheric pressure), 1.8, and the maximum pressure of 29.3 MPa, first in increasing steps and then in five decreasing steps. We determined the effective pressure corresponding to a confining pressure of 1.8 MPa to be 1.7 MPa by subtracting pore pressure, which corresponds approximately to the in situ effective lithostatic pressure of sample TC1. The effective pressure corresponding to the highest experimental confining pressure of 29.3 MPa is roughly equivalent to that at 3 km depth. The thermal conductivity of sample TC1 clearly increased with increasing confining pressure and decreased with decreasing confining pressure (Figure 6a). However, we observed hysteresis; that is, the thermal conductivity at 0.1 MPa after pressure loading

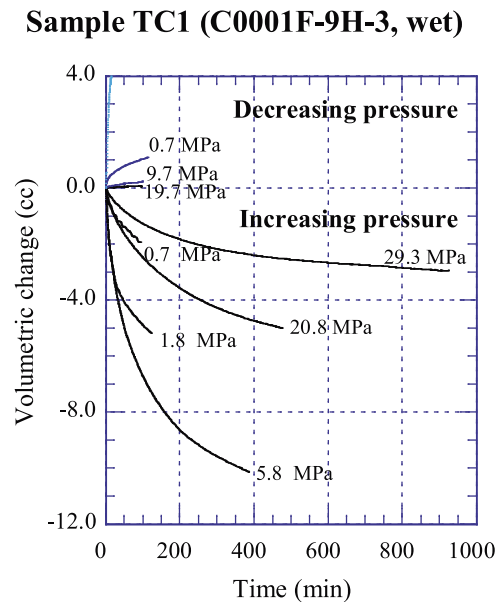


Figure 5. Examples of temporal volumetric changes of NanTroSEIZE sample TC1 (wet) at different constant confining pressures. The volumetric changes were determined from the mass of drained water. A negative volumetric change indicates contraction of the sample; a positive volumetric change indicates expansion. Curves showing negative volumetric changes are from data recorded during stepwise increases of confining pressure (simulating subsidence and compaction); curves showing positive volumetric changes are from data during stepwise decreases of pressure (simulating uplift).

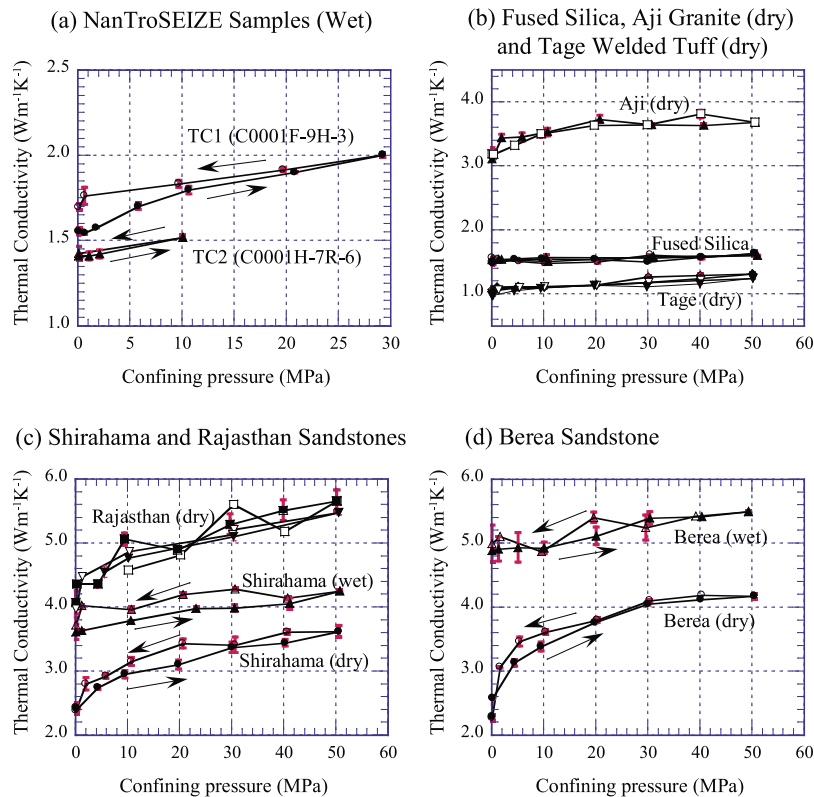


Figure 6. Relationship between thermal conductivity and confining pressure for all samples tested. We measured thermal conductivity two or three times at each pressure. Symbols show average thermal conductivity at each pressure; error bars show the range of values. Solid symbols are for stepwise increasing pressure; open symbols are for stepwise decreasing pressure. Arrows indicate the loading path for stepwise changes of confining pressure.

and subsequent unloading was higher than that at the start of the cycle. During the increase of confining pressure, the gradient of the thermal conductivity curve decreased as confining pressure increased. *Morin and Silva* [1984] also showed a similar correlation of thermal conductivity and pressure for soft ocean sediments.

[19] The thermal conductivities of samples TC1 and TC2 at confining pressures of 1.8 and 2.1 MPa, respectively, corresponding to their in situ pressures, were approximately 2% higher than those at atmospheric pressure. This small difference was because samples TC1 and TC2 came from relatively shallow depths where the pressure effect on thermal conductivity is small.

[20] Generally, thermal conductivity of sediments and rocks at water saturated state may dependent on multiple parameters including mineral composition, porosity and pore geometry. With increasing confining pressure, the porosity may change but the mineral composition may not change in such short time scale as our laboratory tests. For two-phase thermal conductivity models of matrix-water mix-

ture, the following equation called geometric mean model has been widely used [*Pribnow and Sass*, 1995]:

$$\lambda_b = \lambda_s^{(1-\Phi)} \lambda_f^\Phi, \quad (2)$$

where λ_b is bulk thermal conductivity of the matrix-water mixture corresponding to the measured thermal conductivity; λ_s and λ_f are thermal conductivity of solid and fluid, respectively; Φ is the porosity. This equation can be rewritten as:

$$\log_{10} \lambda_b = \log_{10} \lambda_s - \Phi(\log_{10} \lambda_s / \lambda_f), \quad (3)$$

Thus, $\log_{10} \lambda_b$ can be considered to be a linear function of porosity through two material constants λ_s and λ_f . Relation between the measured thermal conductivity and porosity predicted by volumetric change of TC1 sample under high confining pressures showed good consistency with the model (straight line) when increasing confining pressure, but slightly deviated when decreasing confining pressure (Figure 7). Porosity decreased from its initial value of 57% at atmospheric pressure to 22% under confining pressure 29.3 MPa (Figure 7).

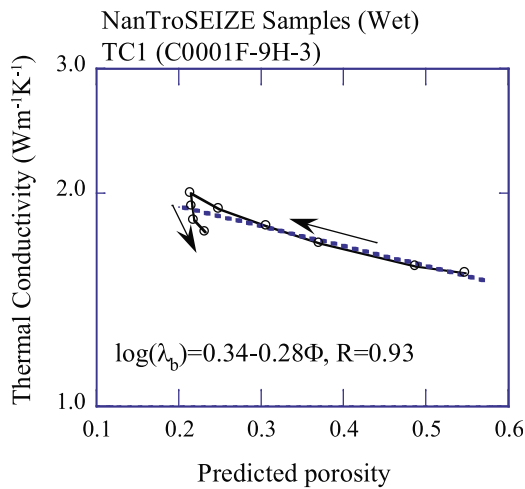


Figure 7. Relationship between thermal conductivity and predicted porosity under confining pressure for NanTroSEIZE sample TC1 (wet) in semilog scale. Dashed line and equation are linear regression line and its equation; R is the correlation coefficient. “ λ_b ” in the equation is measured bulk thermal conductivity, “ Φ ” is the porosity under high confining pressure predicted from initial porosity of the sample and volumetric change data shown in Figure 5. Arrows indicate the loading path for stepwise changes of confining pressure.

Porosity is the fraction of entire volume part occupied by pores, cracks etc. to bulk volume of a sample [Schön, 1998b]. Both of the pores and cracks or microcracks may contract and/or close and make porosity to reduce although the cracks may close more easily than that the pores contract. Therefore, the thermal conductivity change with increasing confining pressure might be caused by change of both the pores and cracks (Figure 7 and equations (2) and (3)). Probably, influences by these two types of interstices are hard to separate without the individual volumetric change data of pores and cracks with increasing pressure.

4.2. The Other Samples

[21] The compressional and shear wave velocities of fused silica tested are 5.71 and 3.45 km/s, respectively. Thus, its Young’s modulus determined from these velocities and its density (2.2 g/cm^3) is very high (99.5 GPa). Because the fused silica is very hard to deform, changes of confining pressure have almost no effect on thermal conductivity (Figure 6b and Figure 4). This result indicates that our thermal conductivity measurements were not influenced by the high pressures except the pressure effects on thermal conductivity of samples. This poor correlation of thermal conductivity and confining pressure for fused silica was almost same as previous

results [Horai and Susaki, 1989; Abdulagatov et al., 2000]. Moreover, the thermal conductivity value of fused silica of this study was almost equal to the upper value of the range $1.31 \pm 0.18 \text{ Wm}^{-1}\text{K}^{-1}$ which was the average and standard deviation of thermal conductivity values reported in literatures on fused silica at room temperature and atmospheric pressure [Horai and Simons, 1969; Horai and Susaki, 1989].

[22] The thermal conductivity of the dry Aji granite sample increased with increasing confining pressure, but the rate of increase decreased with increasing pressure (Figure 6b). Granites generally contain numerous microcracks, even for fresh and intact samples [e.g., Lin, 2002]. It is possible that the microcracks close mainly at the lower pressure range, which would explain the decrease of the rate of thermal conductivity change with increasing pressure. This trend is similar to the findings of several previous experimental studies for granites and granulites [Walsh and Decker, 1966; Seipold, 1992; Kukkonen et al., 1999; Abdulagatov et al., 2006].

[23] The pressure dependencies of thermal conductivity for dry samples of Rajasthan, Shirahama and Berea sandstones were similar (Figures 6c and 6d), and also similar to those of several previous studies for dry sandstones [Woodside and Messmer, 1961; Demirci et al., 2004; Abdulagatov et al., 2006; Abdulagatova et al., 2009]. However, the thermal conductivities for each rock type were different, reflecting their different mineral compositions, porosities, environments of deposition, and geological ages.

[24] Two water-saturated samples of Shirahama and Berea sandstones showed a similar relationship of thermal conductivity to pressure. This monotonous increasing relationship was similar to those of the dry samples, but the rate of thermal conductivity change was lower (Figures 6c and 6d). In addition, the steep changes of thermal conductivity we observed for the dry samples of the two sandstones at pressures lower than 10 MPa were not observed for the wet sandstone samples. For each sandstone, the thermal conductivities of the wet samples were clearly higher than those of the dry samples for the same pressure conditions. Differences between the thermal conductivities of the wet and dry samples of Berea sandstone at the same pressure were larger than those of the Shirahama sandstone samples. This difference might reflect the higher porosity of the Berea sandstone (19.7%) than that of the Shirahama sandstone (13.5%).

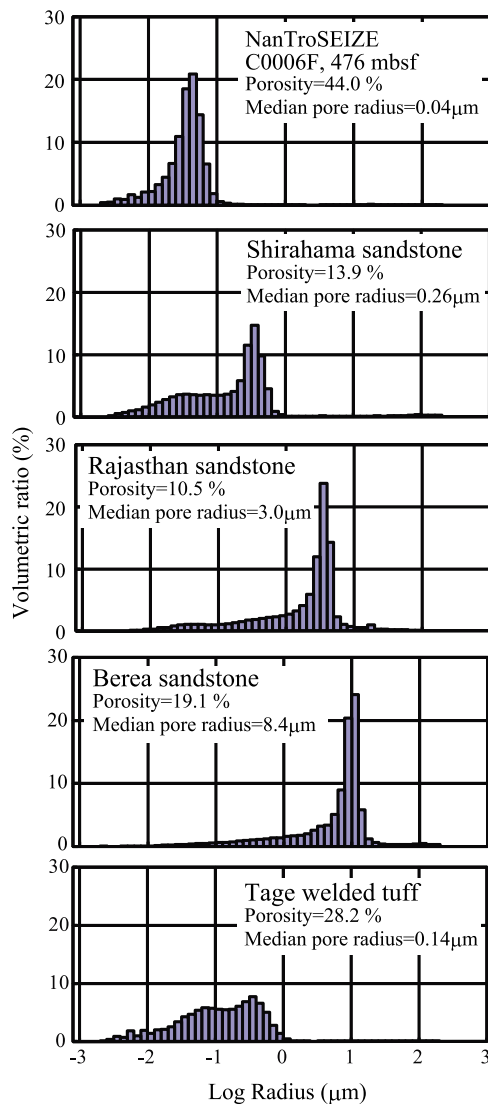


Figure 8. Pore size distributions of various samples determined by mercury intrusion porosimetry [ASTM, 1999]. The NanTroSEIZE sample shown here was from drilling site C0006F, 476 m below seafloor (TC1 and TC2 were from site C0001); the other data are from the same rock block samples also used to measure thermal conductivity. For determination of the pore size distribution, pores were assumed to be cylindrical. Porosity values in these images were determined by mercury porosimetry, and differ from the values mentioned in text, which were determined by the buoyancy method [Franklin, 1979]. The data for the NanTroSEIZE core sample from C0006F and Berea sandstone are from Lin et al. [2010b].

[25] The effect of pressure on thermal conductivity for the dry Tage welded tuff sample was much weaker than for the other rock samples (Figure 6b). Moreover, the thermal conductivities of the tuff were much lower than those of the other rocks. Repeat measurements confirmed the original results

for the tuff, suggesting that the characteristics that control thermal conductivity of the tuff were different from those of the other samples. The tuff had a higher porosity than the sandstones, but the median pore size of the tuff determined by mercury intrusion porosimetry [American Society for Testing and Materials (ASTM), 1999] was smaller than those of the sandstones (Figure 8). The pore structure (lower pore size distribution) and mineral composition (presence of numerous clay minerals including smectite) of the tuff may also have contributed to its markedly lower thermal conductivity and muted thermal conductivity changes in response to increasing pressure.

5. Rate of Change of Thermal Conductivity With Pressure

[26] To quantitatively examine the pressure effect on bulk thermal conductivity (λ_b), we defined the rate of thermal conductivity change with confining pressure (CP) as

$$d\lambda_b/dp = (\lambda_{b2} - \lambda_{b1}) / (CP_2 - CP_1). \quad (4)$$

We calculated a representative rate for each sample by linear regression analysis during pressure loading and then plotted those rates versus porosity (Figure 9). For the regression analysis, we used the thermal conductivities measured in the confining pressure range from approximately 10 to 50 MPa only for the samples loaded up to 50 MPa,

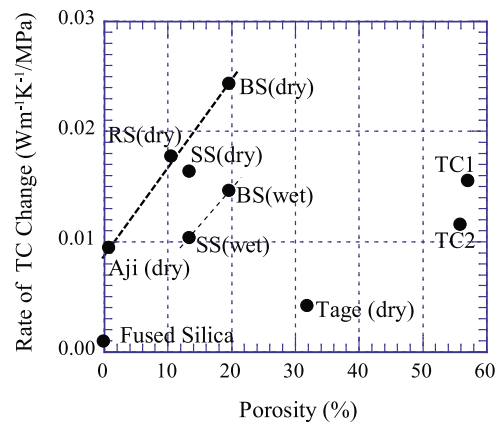


Figure 9. Relationship between porosity and rate of change of thermal conductivity per unit change (MPa) of confining pressure. RS, Rajasthan sandstone; SS, Shirahama sandstone; BS, Berea sandstone. The dark dashed line suggests a positive correlation for dry rocks. The light dashed line indicates a possible positive correlation for wet rocks, but lacks sufficient data.

because the rate was much higher in the lower pressure range (Figures 6b–6d).

[27] For the two wet NanTroSEIZE samples, the rate of thermal conductivity change was $0.012\text{--}0.016\text{ Wm}^{-1}\text{K}^{-1}/\text{MPa}$ for the pressure-loading run, but around $0.01\text{ Wm}^{-1}\text{K}^{-1}/\text{MPa}$ for the pressure-unloading run. Therefore, if we assume an average density of the sediments and rocks of 2.0 g/cm^3 , the depth (pressure) effects are $0.14\text{ Wm}^{-1}\text{K}^{-1}/\text{km}$ for subsidence and $0.1\text{ Wm}^{-1}\text{K}^{-1}/\text{km}$ for uplift. Measurements of thermal conductivities at atmospheric rather than in situ pressure may underestimate thermal conductivity for core samples from large depth. Considering that retrieval of a core sample from depth by drilling releases the original in situ pressure, we can estimate the degree of the underestimation by using $0.1\text{ Wm}^{-1}\text{K}^{-1}/\text{km}$ determined from the pressure-unloading run. Because the measured thermal conductivity of the NanTroSEIZE samples was approximately $1.5\text{ Wm}^{-1}\text{K}^{-1}$, the measurement error at atmospheric pressure may reach 7% for a core sample from 1 km depth, or 20% for a core sample from 3 km depth.

[28] *Expedition 316 Scientists* [2009] tried to correct pressure effect on thermal conductivity at the sites C0004, C0006, C0007, and C0008 measured under atmospheric pressure in onboard laboratory of *D/V Chikyu* by +1% for each 1800 mbsf based on a previous research [Ratcliffe, 1960]. However, this percentage was determined from only an estimation of increasing of thermal conductivities of solid and fluid, but the porosity change with pressure change was not taken into consideration. Influence by the latter (porosity change) may be stronger than that of the former. Thus, the correction by +1% increase in thermal conductivity for each 1800 mbsf may be low. A compilation and analysis of all thermal conductivity measurements from Expeditions 315 and 316, including new divided bar measurements of thermal conductivity, though none at elevated pressures or temperatures, has recently been submitted (R. N. Harris et al., Heat flow along the NanTroSEIZE transect: Results from IODP Expeditions 315 and 316 offshore the Kii Peninsula, Japan, submitted to *Geochemistry Geophysics Geosystems*, 2011.).

[29] We recognized a clear positive correlation between porosity and the rate of thermal conductivity change with pressure for all of the dry samples except the Tago welded tuff (Figure 9). The higher the porosity of dry samples, the higher the rate of thermal conductivity change with pressure. A similar relation was also recognized for the wet

Shirahama and Berea sandstone samples. However, the wet NanTroSEIZE samples (TC1 and TC2) showed low rates of change, despite their high porosities. The median pore radius determined by mercury intrusion porosimetry for a similar NanTroSEIZE sample from a different location (C0006F, 476 mbsf) was very small ($0.04\text{ }\mu\text{m}$), even smaller than that of the Tago welded tuff (Figure 8). This may explain why the rates of thermal conductivity change with pressure for the wet NanTroSEIZE samples were relatively lower, and why there was a poor correlation between the rate and porosity for the wet sandstone and NanTroSEIZE samples (Figure 9). More data are required to derive a reliable correlation between porosity and the rate of thermal conductivity change with pressure for wet rocks. However, our data for the Shirahama and Berea sandstones (Figure 9) clearly show that, for the same type of rock, the rate of thermal conductivity change with pressure for a dry sample is higher than that for a wet sample.

6. Conclusions

[30] We developed an apparatus to measure thermal conductivity of sediment and rock samples at high pressures, thus simulating in situ lithostatic and pore pressures. We examined the relationship of the thermal conductivity to pressure for core samples retrieved from drilling site C0001 of the IODP NanTroSEIZE and for other samples of five terrestrial rock types. We applied pressures of up to 30 MPa for the NanTroSEIZE samples and up to 50 MPa for the other rocks. If the average density of sediments and rocks is assumed to be 2.0 g/cm^3 , a confining pressure of 30 MPa with pore pressure of 0.1 MPa is approximately equivalent to the effective pressure at 3 km depth.

[31] The thermal conductivity of our samples clearly increased with increasing confining pressure. The rate of thermal conductivity change for the NanTroSEIZE samples was around $0.014\text{ Wm}^{-1}\text{K}^{-1}/\text{MPa}$ when pressure was increased (simulating subsidence) and around $0.01\text{ Wm}^{-1}\text{K}^{-1}/\text{MPa}$ when pressure was decreased (simulating uplift). We estimated that the errors in measurements of thermal conductivity at atmospheric rather than in situ pressures may reach 7% for core samples from around 1 km depth or 20% for core samples from around 3 km depth. Our results suggest that it is important to measure thermal conductivities of core samples from great depths under in situ pressure conditions.

[32] In general, we found that the rate of thermal conductivity change with increasing pressure showed a positive correlation with porosity; that is, the pressure effect on thermal conductivity was stronger for more porous material. Clearly, the relation between the rate of thermal conductivity change and porosity is also dependent on the fabric, mineral composition, and pore structure of sedimentary rocks. In addition, for two sandstones we tested, the rates of thermal conductivity change with increasing pressure were higher for dry samples than for wet (water saturated) samples.

[33] In this study, we have not taken into account the effects of temperature on thermal conductivity. We are currently planning further experiments to address both in situ pressure and temperature conditions at depth.

Acknowledgments

[34] The core samples used in this study were provided by the NanTroSEIZE stage 1 program of the IODP. We gratefully acknowledge James Tyburczy, the editor of *G-Cubed*, and Robert N. Harris, the reviewer, for their detailed and constructive comments which helped us to improve this manuscript. We also thank Tetsuro Hirono and Akito Tsutsumi for their useful discussions during the planning of this study, and Daisaku Sato for his help with operation of the mercury intrusion porosimeter. This work was partly supported by Grants-in-Aid for Scientific Research 22403008 (Japan Society for the Promotion of Science, JSPS) and 21107006 (Ministry of Education, Culture, Sports, Science and Technology, MEXT), Japan.

References

- Abdulagatov, I. M., S. N. Emirov, T. A. Tsomaeva, K. A. Gairbekov, S. Y. Askerov, and N. A. Magomedova (2000), Thermal conductivity of fused quartz and quartz ceramic at high temperatures and high pressures, *J. Phys. Chem. Solids*, *61*, 779–787, doi:10.1016/S0022-3697(99)00268-1.
- Abdulagatov, I. M., S. N. Emirov, Z. Z. Abdulagatova, and S. Y. Askerov (2006), Effect of pressure and temperature on the thermal conductivity of rocks, *J. Chem. Eng. Data*, *51*, 22–33, doi:10.1021/je050016a.
- Abdulagatova, Z., I. M. Abdulagatov, and V. N. Emirov (2009), Effect of temperature and pressure on the thermal conductivity of sandstone, *Int. J. Rock Mech. Min. Sci.*, *46*, 1055–1071, doi:10.1016/j.ijrmms.2009.04.011.
- American Society for Testing and Materials (ASTM) (1999), Standard test method for determination of pore volume and pore volume distribution of soil and rock by mercury intrusion porosimetry, in *1999 Annual Book of ASTM Standards*, vol. 04.08, pp. 588–592, West Conshohocken, Pa.
- Ashi, J., et al. (2008), NanTroSEIZE Stage 1A: NanTroSEIZE megaspill riser pilot, *IODP Prelim. Rep.*, *315*, doi:10.2204/iodp.pr.315.2008.
- Demirci, A., K. Gorgulu, and Y. S. Duruturk (2004), Thermal conductivity of rocks and its variation with uniaxial and triaxial stress, *Int. J. Rock Mech. Min. Sci.*, *41*, 1133–1138, doi:10.1016/j.ijrmms.2004.04.010.
- Expedition 315 Scientists (2009), Expedition 315 Site C0001, in *NanTro-SEIZE Stage 1: Investigations of Seismogenesis, Nankai Trough, Proc. I ODP*, *314/315/316*, doi:10.2204/iodp.proc.314315316.123.2009.
- Expedition 316 Scientists (2009), Expedition 316 methods, in *NanTro-SEIZE Stage 1: Investigations of Seismogenesis, Nankai Trough, Proc. IODP*, *314/315/316*, doi:10.2204/iodp.proc.314315316.132.2009.
- Franklin, J. A. (1979), Suggest methods for determining water content, porosity, density, absorption and related properties and swelling and slake-durability index properties, *Int. J. Mech. Min. Sci. Geomech. Abstr.*, *16*, 141–156.
- Galson, D. P., N. P. Wilson, U. Schari, and L. Rybach (1987), A comparison of divided-bar and QTM methods of measuring thermal conductivity, *Geothermics*, *16*, 215–226, doi:10.1016/0375-6505(87)90001-0.
- Goto, S., M. Yamano, and M. Kinoshita (2005), Thermal response of sediment with vertical fluid flow to periodic temperature variation at the surface, *J. Geophys. Res.*, *110*, B01106, doi:10.1029/2004JB003419.
- Harris, R. N., and K. Wang (2002), Thermal models of the Middle America Trench at the Nicoya Peninsula, Costa Rica, *Geophys. Res. Lett.*, *29*(21), 2010, doi:10.1029/2002GL015406.
- Heki, K., and S. Miyazaki (2001), Plate convergence and long-term crustal deformation in central Japan, *Geophys. Res. Lett.*, *28*, 2313–2316, doi:10.1029/2000GL012537.
- Horai, K. (1981), Thermal conductivity of sediments and igneous rocks recovered during deep sea drilling project Leg 60, *Init. Res. DSDP*, *60*, 807–834.
- Horai, K., and G. Simons (1969), Thermal conductivity of rock-forming minerals, *Earth Planet. Sci. Lett.*, *6*, 359–368, doi:10.1016/0012-821X(69)90186-1.
- Horai, K., and J. Susaki (1989), The effect of pressure on the thermal conductivity of silicate rocks up to 12 kbar, *Phys. Earth Planet. Inter.*, *55*, 292–305, doi:10.1016/0031-9201(89)90077-0.
- Hyndman, R. D., K. Wang, and M. Yamano (1995), Thermal constraints on the seismogenic portion of the southwestern Japan subduction thrust, *J. Geophys. Res.*, *100*, 15,373–15,392, doi:10.1029/95JB00153.
- Kano, Y., et al. (2006), Heat signature on the Chelungpu fault associated with the 1999 Chi-Chi, Taiwan Earthquake, *Geophys. Res. Lett.*, *33*, L14306, doi:10.1029/2006GL026733.
- Kinoshita, M., S. Goto, and M. Yamano (1996), Estimation of thermal gradient and diffusivity by means of long-term measurements of subbottom temperatures at western Sagami Bay, Japan, *Earth Planet. Sci. Lett.*, *141*, 249–258, doi:10.1016/0012-821X(96)00081-7.
- Kinoshita, M., G. Moore, R. von Huene, H. Tobin, and C. Ranero (2006), The Seismogenic Zone Experiment, *Oceanography*, *19*(4), 28–38.
- Kukkonen, I. T., J. Jokinen, and U. Seipold (1999), Temperature and pressure dependencies of thermal transport properties of rocks: Implications for uncertainties in thermal lithosphere models and new laboratory measurements of high-grade rocks in the central Fennoscandian shield, *Surv. Geophys.*, *20*, 33–59, doi:10.1023/A:1006655023894.
- Lachenbruch, A. (1980), Frictional heating, fluid pressure, and the resistance to fault motion, *J. Geophys. Res.*, *85*, 6097–6112, doi:10.1029/JB085iB11p06097.
- Lallemant, S., and F. Funiciello (2009), *Subduction Zone Geodynamics*, Springer, Berlin, doi:10.1007/978-3-540-87974-9.



- Lin, W. (2002), Permanent strain of thermal expansion and thermally induced microcracking in Inada granite, *J. Geophys. Res.*, *107*(B10), 2215, doi:10.1029/2001JB000648.
- Lin, W., et al. (2010a), Present-day principal horizontal stress orientations in the Kumano forearc basin of the southwest Japan subduction zone determined from IODP NanTroSEIZE drilling site C0009, *Geophys. Res. Lett.*, *37*, L13303, doi:10.1029/2010GL043158.
- Lin, W., O. Tadai, M. Takahashi, D. Sato, T. Hirose, and W. Tanikawa (2010b), Comparison of bulk densities and porosities of various rock samples measured by different techniques, in *Geologically Active*, edited by A. L. Williams et al., pp. 2081–2086, Taylor and Francis, London.
- Moore, G., et al. (2007), Three-dimensional spaly fault geometry and implications for tsunami generation, *Science*, *318*, 1128–1131, doi:10.1126/science.1147195.
- Morin, R., and A. J. Silva (1984), The effects of high pressure and high temperature on some physical properties of ocean sediments, *J. Geophys. Res.*, *89*, 511–526, doi:10.1029/JB089iB01p00511.
- Osako, K., E. Ito, and A. Yoneda (2004), Simultaneous measurements of thermal conductivity and thermal diffusivity for garnet and olivine under high pressure, *Phys. Earth Planet. Inter.*, *143–144*, 311–320, doi:10.1016/j.pepi.2003.10.010.
- Park, J.-O., et al. (2002), Splay fault branching along the Nankai subduction zone, *Science*, *297*, 1157–1160, doi:10.1126/science.1074111.
- Pribnow, D., and J. H. Sass (1995), Determination of thermal conductivity from deep boreholes, *J. Geophys. Res.*, *100*, 9981–9994, doi:10.1029/95JB00960.
- Pribnow, D., C. F. Williams, J. H. Sass, and R. Keating (1996), Thermal conductivity of water-saturated rocks from the KTB pilot hole at temperature of 25 to 300°C, *Geophys. Res. Lett.*, *23*, 391–394.
- Ratcliffe, E. H. (1960), The thermal conductivities of ocean sediments, *J. Geophys. Res.*, *65*, 1535–1541.
- Sass, J. H., C. Stone, and R. J. Munroe (1984), Thermal conductivity determinations on solid rock—A comparison between a steady-state divided bar apparatus and a commercial transient line-source device, *J. Volcanol. Geotherm. Res.*, *20*, 145–153, doi:10.1016/0377-0273(84)90071-4.
- Schön, J. H. (1998a), Thermal properties of rocks, in *Physical Properties of Rocks*, 2nd ed., *Handbook of Geophysical Exploration: Seismic Exploration*, vol. 18, chap. 8, pp. 323–378, Pergamon, Amsterdam, Netherlands.
- Schön, J. H. (1998b), *Pore Space Properties: Porosity, Specific Internal Surface, and Permeability*, 2nd ed., *Handbook of Geophysical Exploration: Seismic Exploration*, vol. 18, chap. 2, pp. 23–58, Pergamon, Amsterdam, Netherlands.
- Seipold, U. (1992), Depth dependence of thermal transport properties for typical crustal rocks, *Phys. Earth Planet. Inter.*, *69*, 299–303, doi:10.1016/0031-9201(92)90149-P.
- Seipold, U., and E. Huenges (1998), Thermal properties of gneisses and amphibolites high pressure and high temperature investigations of KTB-rock samples, *Tectonophysics*, *291*, 173–178, doi:10.1016/S0040-1951(98)00038-9.
- Tanaka, H., et al. (2006), Frictional heat from faulting of the 1999 Chi-Chi, Taiwan earthquake, *Geophys. Res. Lett.*, *33*, L16316, doi:10.1029/2006GL026673.
- Villinger, H., I. Grevemeyer, N. Kaul, J. Hauschild, and M. Pfender (2002), Hydrothermal heat flux through aged oceanic crust: Where does the heat escape?, *Earth Planet. Sci. Lett.*, *202*, 159–170, doi:10.1016/S0012-821X(02)00759-8.
- Walsh, J. B., and E. R. Decker (1966), Effect of pressure and saturating fluid on the thermal conductivity of compact rock, *J. Geophys. Res.*, *71*, 3053–3061.
- Wang, K., R. D. Hyndman, and M. Yamano (1995), Thermal regime of the southwest Japan subduction zone: Effects of age history of the subducting plate, *Tectonophysics*, *248*, 53–69, doi:10.1016/0040-1951(95)00028-L.
- Woodside, W., and J. H. Messmer (1961), Thermal conductivity of porous media. II. Consolidated rocks, *J. Appl. Phys.*, *32*, 1699–1706, doi:10.1063/1.1728420.
- Xu, Y., T. J. Shankland, S. Linhardt, D. C. Rubie, F. Langenhorst, and K. Klasinski (2004), Thermal diffusivity and conductivity of olivine, wadsleyite and ringwoodite to 20 GPa and 1373 K, *Phys. Earth Planet. Inter.*, *143–144*, 321–336, doi:10.1016/j.pepi.2004.03.005.
- Yamano, M., M. Kinoshita, S. Goto, and O. Matsubayashi (2003), Extremely high heat flow anomaly in the middle part of the Nankai Trough, *Phys. Chem. Earth*, *28*, 487–497.